https://doi.org/10.21122/2227-1031-2022-21-3-179-190

UDC 621.793:621.365:544.3

Evaluation of Evaporative Degradation of Arc Torch Cathodes in Hydrocarbon-Containing Plasmas for Spraying, Thermal Protection Testing and Related Technologies

A. V. Gorbunov[1)], V. A. Gorbunova[2)], O. G. Devoino[2)], G. Petraconi Filho[1)], A. A. Halinouski[3)]

[1)]Aeronautics Institute of Technology (Sao Jose dos Campos, Brazil),
[2)]Belarusian National Technical University (Minsk, Republic of Belarus),
[3)]Institute of Atmospheric Physics of CAS (Prague, Czech Republic)

Abstract. Design of non-transferred DC electric arc plasma torches (EAPTs) operated with plasma gases containing alkane hydrocarbons, as a promising type of heaters for a number of technologies (thermal spraying, surface hardening, testing of thermal protection systems, etc.), requires taking into account the evaporation rate of surface cathode material (as one of the channels of its ablative degradation). For this procedure, as the first stage, thermodynamic methods can be used to simulate the composition and properties of reactive C–H–O–N–Ar–Me-systems with variable set of such input parameters as the ratio of components of plasma-forming mixture, its pressure and temperature. We theoretically estimated the evaporative degradation of the material for three variants of EAPT cathode with alkane-containing plasmas ("hot" thermochemical zirconium and thermionic tungsten, and "cold" copper) in equilibrium and quasi-equilibrium modes of "plasma gas + surface cathode material"-mixture, with use of generalized thermodynamic properties of the materials. The calculation for conditions with pressure, which is characteristic for EAPT discharge chamber, showed that when varying the initial composition of the plasma-forming mixture (from oxidizers (air or combustion products of alkanes) to reducing gases based on the products of combined partial oxidation and pyrolysis of alkanes), the effect of a difference in the cathode evaporation rate *EAI* was observed in systems based on (air + alkane)-mixtures near the melting point of surface cathode substances, in a comparison with the case of EAPTs with more conventional gases (commercial N_2, air) and, importantly, for two variants of the analyzed cathodes (with the exception of copper). In addition, the electrode erosion value was compared for simulated zirconium cathode (in terms of erosion evaporative component) when operating on the combustion products of alkanes from "air + CH_4"-mixture, and for some known EAPTs with similar cathodes in other gases. Using the case of earlier tested DC plasma torch with rod Zr-cathode (with microheterogeneous surface) as an example, it was found that our calculation indicates non-monotonic dynamics of *EAI* value and fractions of Zr-containing vapors as a result of the change of the fuel-air equivalence ratio ϕ of initial reactive mixture. This effect is inconsistent with measured cathode composition, which shows a probability of nonequilibrium character of thermal and diffusion processes in near-electrode plasma and surface layer (~1 mm) of the electrode, at least in the modes with arc current in the torch near 300 A. Besides this, it should be noted that obtained modeling data on the behavior of zirconium compounds (ZrO_2, ZrC) in C–H–O–N–Ar–Zr-system can be used not only for improvement of the torch cathodes, but also for design of new Zr-containing thermal protection systems to predict preliminary their ablation rate in a flow of products of combustion (including incomplete one) of engine-, rocket- and other fuels. Similarly, the results on the copper compounds behavior near the metal evaporation temperature can be useful for optimizing the process of plasma spraying of copper alloy coatings.

Keywords: electric arc torches, plasma spraying, testing of thermal protection systems, cathode materials, zirconium, tungsten, copper, evaporation, alkane-containing plasmas, thermochemical analysis

For citation: Gorbunov A. V., Gorbunova V. A., Devoino O. G., Petraconi Filho G., Halinouski A. A. (2022) Evaluation of Evaporative Degradation of Arc Torch Cathodes in Hydrocarbon-Containing Plasmas for Spraying, Thermal Protection Testing and Related Technologies. *Science and Technique*. 21 (3), 179–190. https://doi.org/10.21122/2227-1031-2022-21-3-179-190

Адрес для переписки
Горбунова Вера Алексеевна
Белорусский национальный технический университет
просп. Независимости, 67,
220013, г. Минск, Республика Беларусь
Тел.: +375 17 293-92-71
ecology@bntu.by

Address for correspondence
Gorbunova Vera A.
Belarusian National Technical University
67, Nezavisimosty Ave.,
220013, Minsk, Republic of Belarus
Tel.: +375 17 293-92-71
ecology@bntu.by

Оценка испарительной деградации катодов плазмотронов с C_xH_y-содержащими плазмами для напыления, тестирования теплозащиты и смежных технологий

Канд. техн. наук А. В. Горбунов[1)], канд. хим. наук, доц. В. А. Горбунова[2)], докт. техн. наук, проф. О. Г. Девойно[2)], докт. филос. (PhD), проф. Ж. Петракони-фильо[1)], канд. техн. наук А. А. Галиновский[3)]

[1)]Технологический институт аэронавтики (Сан-Жозе-дус-Кампус, Бразилия),
[2)]Белорусский национальный технический университет (Минск, Республика Беларусь),
[3)]Институт физики атмосферы Академии наук Чешской Республики (Прага, Чешская Республика)

Реферат. Разработка электродуговых плазмотронов (ЭДП) на плазмообразующих газах с алкановыми углеводородами (АУВ) как перспективной разновидности плазмотронов косвенного действия для ряда технологий (в том числе напыления покрытий, тестирования теплозащитных материалов и др.) требует учета скорости испарения материала катодов (как одного из каналов их абляционной деградации). Для этой процедуры в качестве первой стадии может быть использовано моделирование состава и свойств реагирующей системы типа C–H–O–N–Ar–Me термодинамическим методом при варьируемых входных параметрах – соотношении компонентов в плазмообразующей смеси, ее давлении и температуре. Авторы теоретически оценивали испарительную деградацию материалов в трех вариантах катода ЭДП с АУВ-содержащими плазмами («холодный» из меди и тугоплавкие «горячие» – термохимический из циркония и термоэмиссионный из вольфрама) в квазиравновесном и равновесном режимах смеси «плазмообразователь + материал поверхности катода» с учетом обобщенных данных по фазовым переходам в данных материалах. Расчет для условий с характерным для разрядной камеры ЭДП давлением показал, что изменение состава плазмы (от окислителя (смесь продуктов сгорания АУВ) до восстановителя из продуктов комбинации частичного окисления и пиролиза АУВ) дает явный эффект отличия интенсивности испарения катода *EAI* вблизи точки плавления вещества его поверхности в воздушно-алкановых средах по сравнению с вариантом ЭДП на более простых газах (техническом N_2, воздухе), причем для двух вариантов катода (за исключением меди). Сопоставлен уровень эрозии (рассчитанный по испарительной составляющей) циркониевого катода в среде продуктов сгорания АУВ (из смеси «воздух + CH_4») и этот же параметр, но в опытах с известными ЭДП со сходными катодами в других газах. На примере ранее изученного ЭДП со стержневым катодом из Zr с гетерогенной поверхностью показано, что термохимический расчет дает немонотонное изменение параметра *EAI* и концентраций Zr-содержащих паров при сдвиге фактора эквивалентности ϕ плазмообразующей смеси. Такой эффект не согласуется с найденным в эксперименте составом катода, что указывает на вероятность неравновесного характера тепловых процессов и диффузии в приэлектродной плазме и в поверхностном слое (~1 мм) катода, по крайней мере, в режимах с силой постоянного тока в дуге ЭДП около 300 А. Полученные в расчете данные о поведении соединений ZrO_2 и ZrC в системе C–H–O–N–Ar–Zr можно применять не только для оптимизации катодов плазмотронов, но и в разработке новых Zr-содержащих керамических теплозащитных систем, в том числе для прогноза темпа их разрушения в потоках продуктов сгорания (в том числе неполного) моторных, ракетных и иных топлив. Сходным образом результаты по поведению меди вблизи температуры ее испарения могут быть полезны для совершенствования процессов газотермического напыления покрытий из сплавов меди.

Ключевые слова: дуговые плазмотроны, плазменное напыление, тестирование теплозащитных материалов, катодные материалы, цирконий, вольфрам, медь, испарение, углеводородсодержащие плазмы, термохимический расчет

Для цитирования: Оценка испарительной деградации катодов плазмотронов с C_xH_y-содержащими плазмами для напыления, тестирования теплозащиты и смежных технологий / А. В. Горбунов [и др.] // *Наука и техника*. 2022. Т. 21, № 3. С. 179–190. https://doi.org/10.21122/2227-1031-2022-21-3-179-190

Introduction

The field of application of thermal plasma heaters, in particular the most efficient and industrially commonest type of them – DC electric arc plasma torches (EAPTs) operating at atmospheric pressure (i. e. under conditions close to thermodynamic equilibrium) – is quite wide and includes surface engineering, thermal protection testing, plasma chemical synthesis and processing of inorganic and organic powder materials and chemical products, pyrolysis, gasification and decomposition of industrial and municipal wastes, plasma-fuel technologies, etc. [1–3]. One of the promising variants of such torches is a group that uses not individual plasma-forming gases, but

oxidizer-fuel mixtures, in particular, based on air with natural or liquefied petroleum gases (mainly contain alkanes C_nH_{2n+2}) [3–7].

The previously demonstrated areas for engineering application of the torches with plasmas based on hydrocarbons and combined plasma-fuel systems of atmospheric pressure with near-equilibrium plasmas are the following:

1) plasma spraying (APS) of ceramic and some metal coatings, including RPS, operating with powder and other feedstock [3–6];

2) hardening of steels and alloys surface by the plasma jets similar to the standard case-hardening type [7].

It is also quite obvious that the use of this type of thermal plasma heaters and combined equipment based on these is also possible in the following areas:

a) coating deposition in the hybrid plasma-fuel spraying systems with powder or wire materials by analogy with the approach of the authors [8, 9];

b) testing of ablative destruction of ceramic and composite thermal protection materials/systems (for aerospace, gas turbine and rocket technologies) under the temperature and dynamic action of plasma jets, by analogy with performed plasma and flame tests of such materials [10–13];

c) in the units for thermal vitrification of ash silicate (including dispersed) wastes [14];

d) in thermal apparatuses/furnaces of power engineering sector to suppress the formation of NO_x during the oxidation of gaseous and other fuels, as, for example, in the research [15];

e) in technology of surface melting of ceramic and other coatings and pressurized products, by analogy with the laser or plasma approach [16].

Non-transferred arc DC plasma torches suitable for use in these technologies can be efficiently operated with plasma gases containing of alkane hydrocarbons (AHCs), including natural gas or liquefied petroleum gas [3–7]. Herewith during their development, it is required as one of the most important parts to take into account the rate of vaporization of the material of their cathode (typically metal), as one of the main channels of its degradation during the temperature and dynamic induced ablation in plasma flows [1–3, 17, 18]. For these torches the intensity of electrode erosion is quite important, especially for cathodes, because it directly determines the electrode lifetime. For this analysis procedure the modeling of the atomic and molecular composition and thermophysical properties of reactive system of the C–H–O–N–Ar–Me-type can be used, as the first stage, with conventional thermodynamic methods. Wherein it is advisable to consider theoretically the character of evaporative decomposition of the material with the comparing such three typical variants of cathode of the torches with AHC-containing plasmas as “cold” copper and refractory “hot” thermionic tungsten and thermochemical zirconium. For non-transferred arc DC plasma torches the intensity of electrode erosion is quite important, together with other parameters, especially for cathodes, because it directly determines the electrode lifetime. Under such analysis, the output parameters of a chemically reactive system are usually obtained at a varied level of input parameters, such as the ratio of initial components in the plasma-forming mixture, its pressure and mass averaged temperature in the thermodynamic equilibrium or quasi-equilibrium regimes [3, 15, 19, 20].

Modeling approach

The variant of thermodynamic calculation method was used, which is based on finding the maximum of entropy of reactive system (i. e. minimization of the Gibbs free energy/thermodynamic potential) in the considered equilibrium or quasi-equilibrium systems, at specified pressure and temperature at the inlet, using such code for chemical thermodynamic analysis as TERRA, which was developed in MSTU, Moscow [19].

Schematic diagrams of the examples of DC EAPTs with the considered type of refractory metal cathodes for thermal spray systems and related technologies [17, 18, 21] are shown in Fig. 1. Typical operating pressure p in gas discharge chambers of the torches of this type is near 0.2 MPa [3, 22]. Herewith the typical difference of the composition in many analyzed equilibrium systems of the C–H–O–N–Ar–Zr-type when their pressure is changing in the range near the value of 0.2 MPa was found to be quite small (Fig. 2).

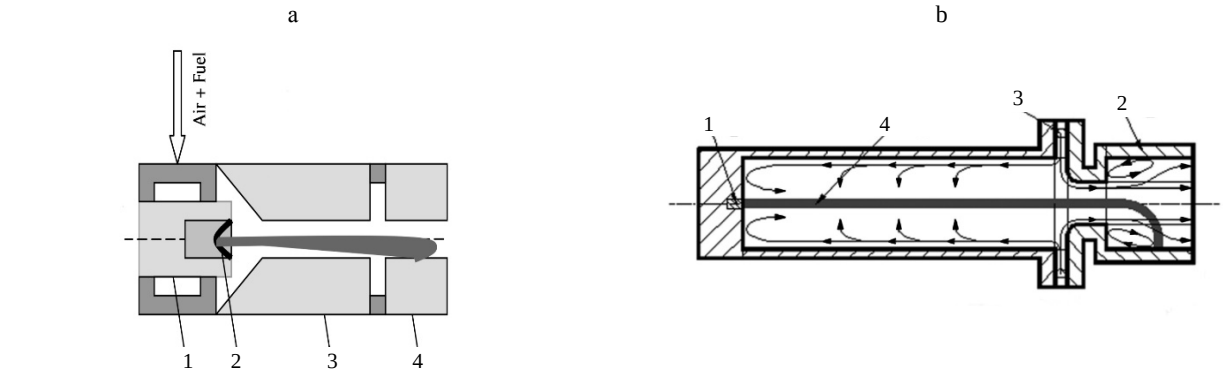

Fig. 1. Schematics of some DC non transferred arc plasma torches with metal cathodes for thermal spraying, surface hardening and other technologies: a – experimental plasma torch with thermo-chemical cathode [17, 18]: 1 – cathode; 2 – button-type insertion (Zr rod) of the cathode; 3 – electrically neutral diaphragm; 4 – anode; b – pilot-scale plasma torch with reverse gas vortex and thermo-chemical cathode [21]: 1 – button-type insertion of the cathode (Zr or Hf); 2 – anode; 3 – gas vortex chamber; 4 – electric arc column

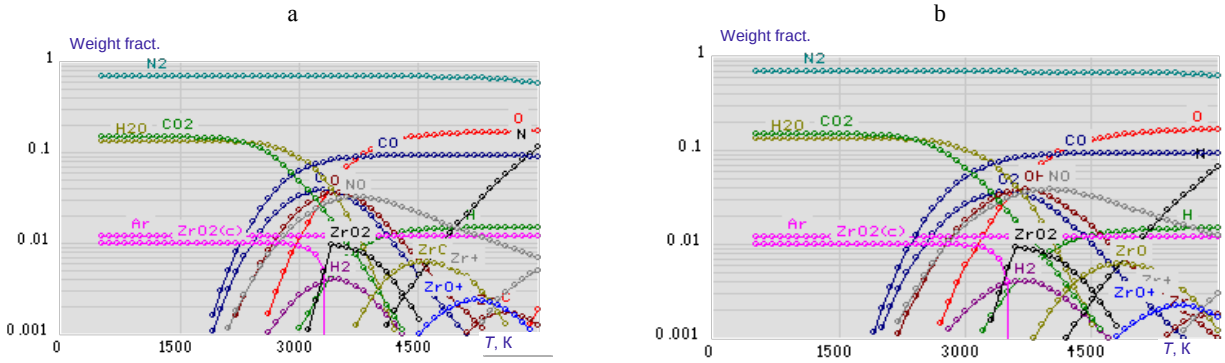

Fig. 2. Calculated composition (in weight fractions) of equilibrium C–H–O–N–Ar–Zr-system, based on the "air + CH_4"-mixture, at the temperature range T = 500–6000 K at the ratio of mass rates of initial Me-containing part (taken as dioxide ZrO_2) to initial "air + CH_4"-part as 1 to 100 at the value of fuel to air equivalence ratio ϕ = 1.0 (i. e. stoichiometric combustion regime) at pressure p: a – 0.101 MPa; b – 0.303 MPa

Results of the modeling

For analysis of degradation of the cathodes of the AHC-operated torches, as the first approach, it is advisable to consider the rate of evaporation of the material of their surface layer with thermodynamic approximation as a set of isothermal sections for initial plasma-forming mixture with its variable composition on the hydrocarbon (C_xH_y) fraction. For three main variants of the torch cathodes the character of the evaporative component of the degradation of their surface material was theoretically considered in the regimes of thermodynamic equilibrium and quasi-equilibrium for "plasma gas + cathode material"-system.

The calculations (Fig. 3–9, Tab. 1–4) showed that when varying the initial composition of the plasma-forming mixture (in the range from oxidezing gases (air or alkane combustion products) to reducing gases formed by the products of simultaneous partial oxidation (POX) and pyrolysis of alkanes (CH_4, LPG, etc.)), the effect manifested itself at the temperatures near the melting point of cathode surface. This indicates the difference in the values of cathode mass losses (i. e. evaporative ablation intensity *EAI*) in the systems based on "air + alkane"-mixtures in a comparison with "background" case of more simple plasma gases (air or N_2 of technical quality) for two (Zr and W) of the three variants of the cathodes. This shows the advisability of taking this factor into account in the further development of the torches using this group of reactive plasma gases.

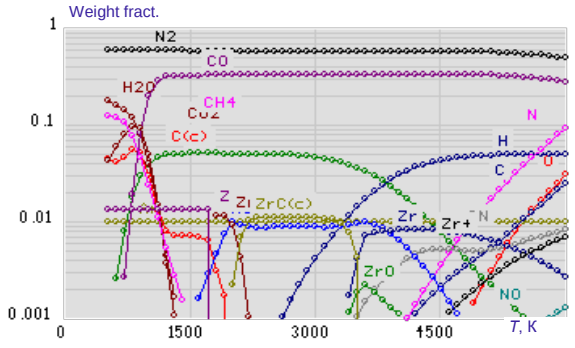

Fig. 3. Composition (in weight fractions) of equilibrium C–H–O–N–Ar–Zr-system, based on the "air + CH_4"-mixture with fuel to air equivalence ratio ϕ = 4.39 (Tab. 3), at the range T = 500–6000 K (at p = 0.202 MPa) at the ratio of mass rates of initial Me-containing part (taken as metal Zr) to initial gaseous part as 1 to 100; this regime is the bound one to appear the condensed zirconium carbide state in the system

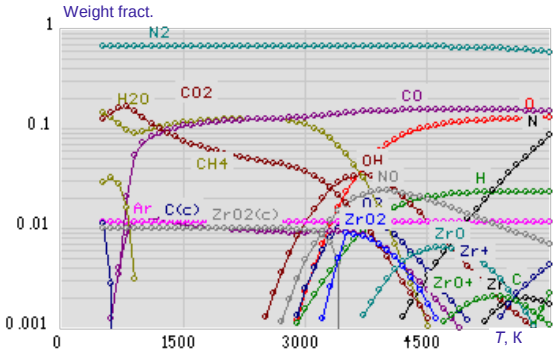

Fig. 4. Composition (in weight fractions) of equilibrium C–H–O–N–Ar–Zr-system, based on the "air + CH_4"-mixture with the ratio ϕ = 1.71 (Tab. 1), at the range T = 500–6000 K (at p = 0.202 MPa) at the ratio of mass rates of initial Me-containing part (taken as dioxide ZrO_2) to initial gaseous part as 1 to 100

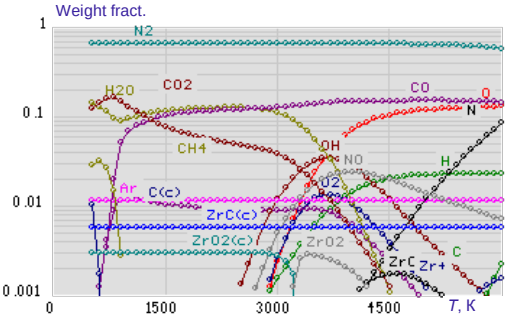

Fig. 5. Composition (in weight fractions) of quasi-equilibrium C–H–O–N–Ar–Zr-system, based on the "air + CH_4"-mixture with the ratio ϕ = 1.71, at the range T = 500–6000 K (at p = 0.202 MPa) at the ratio of mass rates of initial Me-containing part (taken as ZrO_2) to initial gaseous part as 1 to 100; this regime uses the fixation of condensed zirconium carbide in the system (at 3100 K) with the same fraction as was experimentally found [17, 18] in the torch' Zr-cathode surface in the regime No 3 (Tab. 1)

Table 1

Experimental data and additionally calculated parameters for the operating regimes of button-type Zr-cathode of DC plasma torch with group of "air + CH_4"-based plasmas [17, 18]

Operating regime	Mass fraction of the CH_4 in input plasma gas, kg/kg	Thickness of formed emission layer on the torch cathode δ, mm	Mole fraction of oxygen in the cathode layer, %	Mole fraction of carbon in the cathode layer, %	Fuel to air equivalence ratio for plasma gas ϕ	Mass fraction of ZrO_2 phase in the cathode layer, %	Mass fraction of ZrC phase in the cathode layer, %	Ratio of mass fractions of ZrC and ZrO_2 phases in the cathode layer, kg/kg
1	0	0.9	34.0	0	$\approx 10^{-4}$	58.44	0	0
2	0.10	1.3	29.5	7.0	1.077	50.93	13.50	0.265
3	0.15	1.1	14.0	30.0	1.711	24.61	58.91	2.394

The Tab. 2 demonstrates some characteristics of the considered cathode materials, which are important for the evaluation of evaporative degradation at ablation of the materials under the high temperature operation.

In the Tab. 1 the data are presented for the part of experimental parameters of the button-type zirconium cathode in DC plasma torch with group of "air + CH_4"-plasmas [17, 18] and additionally calculated characteristics for these regimes to demonstrate composition of the cathode after the operation in this AHC-type plasma.

Using our analysis with an example for the case of tested in [17, 18] "CH_4 + air"-operated torch with the Zr-cathode with heterogeneous surface layer, it was shown that the calculations in equilibrium

and quasi-equilibrium approximations predict the nonlinear behavior of the cathode degradation parameter *EAI* and the concentrations of Zr-containing vapors in gas phase, depending on a value of the equivalence ratio ϕ for plasma-forming mixture in terms of C_xH_y-fraction in this.

Table 2

Some physical properties of analyzed cathode materials (metals and possible compounds after chemical interaction with plasmas) for the plasma torches with AHC-containing plasmas, based on referenced data and the values from thermodynamic database, used in TERRA-code [19, 23]

Properties (for phase changes – typically at ambient pressure) ↓	Commercial ThO_2-doped (2 wt. %) tungsten	Zr	Cu
Molecular weight, kg/mol	0.18384 (W); 0.18480 (W + Th); 0.19585 (WC); 0.19585 (W_2N) [24]	0.091224 (Zr); 0.123223 (ZrO_2 – CAS number [1314-23-4]); 0.103235 (ZrC); 0.105231 (ZrN) [24]	0.063546 (Cu); 0.079545 (CuO); 0.143091 (Cu_2O) [24]
Melting point T_m, K	3680–3695 (W) [25–27]; 2023 (Th) [25]; 3058–3093, 3053 (WC – CAS number [12070-12-1]) [25, 28–30]	2125–2128 (Zr) [25, 26]; 2950–2983, 2963 (ZrO_2) [25, 31–33]; 3805–3700, 3845, 3673 (ZrC – CAS number [12070-14-3]) [25, 34–37]; 3233, 3228±30 (ZrN – CAS number [25658-42-8]) [25, 38]	1358 (Cu) [24, 25]; 1599–1719 (CuO – CAS number [1317-38-0]) [25, 31]; ~1517 (Cu_2O) [24]
Value of T_m used in TERRA data base, K	3695 (W); 3050 (WC) and 3050 (W_2C)	2133 (Zr); 2983 (ZrO_2), 3700 (ZrN) and 3720 (ZrC)	1358 (Cu); 1517 (Cu_2O) and 1700 (CuO)
Boiling point T_b, K	5828–5933 (W) [25, 26]; 5061 (Th) [25]; 6273 (WC) [28, 30]	4682–3851 (Zr) [25, 26]; 4300–4330 (ZrO_2) [39, 40]; 5370 (ZrC) [41]	2835–2840 (Cu) [25, 26]; 2170–2270 (CuO) [40, 42]
Electron work function Φ of the metals and their compounds, eV	4.32 (W{116}–W{110}); 2.40 (polycrystalline Th) [25]; 3.05–3.47 ("W + 2 % ThO_2"-phase) [43]; 4.6–5.6 (WC {011}, {111}) [44]	4.05 (polycrystalline Zr); 4.02 (ZrC{lattice plane 100}) [45]	4.48–5.10 (Cu{110}–Cu{100}) [25]; 4.84–5.0 (Cu_2O films) and 4.7–5.5 (CuO) [46, 47]
Ionization potential of neutral atom of the metal, eV	7.8640 (W); 6.3067 (Th) [25]	6.6339 **(**Zr) [25]	7.7264 **(**Cu) [25]

Table 3

Calculated parameters for vaporizing Zr-cathode (in metal and oxide forms) with the group of AHC-based plasma gases for the regimes (p = 0.202 MPa) similar to the plasma experimental regimes in [17, 18]

Parameter → Gas medium ↓	100-*EAI* (wt. %) at T_1 = 2900 K	100-*EAI* (wt. %) at T_2 = 3100 K = = 1.069T_1	$MF_{sumZrOx\text{-}vap}$ at T = 2900 K, kg of vapors/(kg of gas phase)	$MF_{sumZrOx\text{-}vap}$ at T = 3100 K, kg of vapors/(kg of gas phase)
1	2	3	4	5
Oxidative plasmas – thermodynamic equilibrium case				
1) Air (composition on [48]) (at the ϕ = 1/*ER* ≈ ≈ 10^{-4}, i. e. the ratio variant as in [20] *ER* ≈ ≈ 10^4 [49]) – Regime #1 from [17, 18]	† (at ZrO_2 in the initial mixture) 99.159	† (at ZrO_2) 95.078	† (at ZrO_2) $8.410 \cdot 10^{-5}$	† (at ZrO_2) $4.916 \cdot 10^{-4}$
2) O_2 (pure, 100 %)	† (at ZrO_2) 99.237	† (at ZrO_2) 95.488	† (at ZrO_2) $7.618 \cdot 10^{-5}$	† (at ZrO_2) $4.508 \cdot 10^{-4}$
Oxidative plasmas – thermodynamic quasi-equilibrium (with fixing of mass fraction of ZrC(c) in the mixture) and equilibrium (without the fixing) cases				
3) Air + CH_4 (at ϕ = = 1/*ER* = 1.0774, i. e. *ER* = 0.9282) – Regime #2 from [17, 18]	† (at ZrO_2) 99.078 / ‡ (with fixing of the fractions of ZrC(c) and ZrO_2(c)): 99.041 {at 500 K, 2900 K, 3100 K exists only ZrO_2(c) phase}	† (at ZrO_2) 94.486 / ‡ (with fixing of the fractions of ZrC(c) and ZrO_2(c)): 94.276	† (at ZrO_2) $9.216 \cdot 10^{-5}$ / ‡ (with fixing of the fractions of ZrC(c) + + ZrO_2(c)): $9.21 \cdot 10^{-5}$	† (at ZrO_2) $5.502 \cdot 10^{-4}$ / ‡ (with fixing of the fractions of ZrC(c) + + ZrO_2(c)): $5.50 \cdot 10^{-4}$

Окончание табл. 3

End of Table 3

4) Air + CH_4 (at ϕ = = 1/*ER* = 1.7111, i. e. *ER* = 0.5844) – Regime #3 from [17, 18]	† (at ZrO_2) 98.969 / ‡ (with fixing of the fractions of ZrC(c) and ZrO_2(c)): 98.832 {at 500 K, 2900 K, 3100 K exists only ZrO_2(c)}	† (at ZrO_2) 93.858 / ‡ (with fixing of the fractions of ZrC(c) and ZrO_2(c)): 93.088	† (at ZrO_2) $1.028 \cdot 10^{-4}$ / ‡ (with fixing of the fractions of ZrC(c) + + ZrO_2(c)): $1.025 \cdot 10^{-4}$	† (at ZrO_2) $6.114 \cdot 10^{-4}$ / ‡ (with fixing of the fractions of ZrC(c) + +ZrO_2(c)): $6.10 \cdot 10^{-4}$
Non-oxidative plasma – thermodynamic equilibrium case				
5) Air + CH_4 (at ϕ = = 1/*ER* = 4.390, i. e. *ER* = 0.2278)	† (at Zr in the initial mixture) 83.496 ≡ 99.663 (for the standardized value (only ZrO_2(c) at 500 K; exists only ZrC(c) at 2900 K and 3100 K)* / (at ZrO_2) 83.952 ≡ 99.228 (for standardized value with the recalculation to pure Zr) – mixture of ZrC(c) + ZrN(c) at 2900 K; only ZrO_2(c) at 500 K	† (at Zr) 81.838 ≡ ≡ 97.683 (for the standardized value (only ZrC(c))** / (at ZrO_2) 79.442 ≡ ≡ 94.351 (for standardized value with the recalculation to Zr) – ZrC(c) + + ZrN(c) at 3100 K	† (at Zr) $3.779 \cdot 10^{-5}$	† (at Zr) $2.541 \cdot 10^{-4}$
Designation: † – thermodynamic equilibrium state; ‡ – thermodynamic quasi-equilibrium state. * ZrO_2(c) → ZrC(c).				

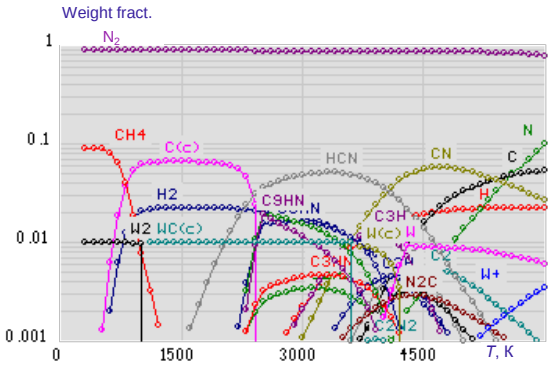

Fig. 6. Composition (in weight fractions) of equilibrium C–H–N–Me-system (Me = (W + ThO_2 (2 wt. %)), based on the commercial "N_2 (high quality [51] + + 10 wt. % CH_4"-mixture, at the range *T* = 300–6000 K (at *p* = 0.202 MPa) at the ratio of mass rates of initial Me-containing part (taken as W + ThO_2) to initial gaseous part as 1 to 100 (Tab. 4)

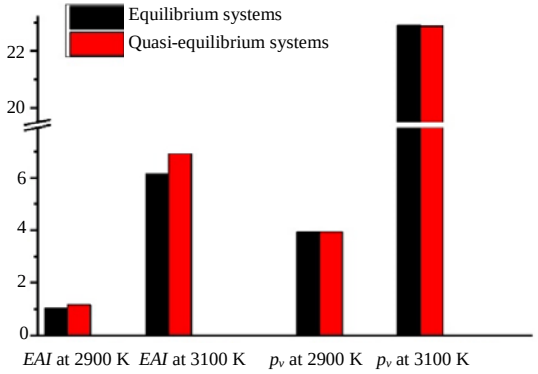

Fig. 7. Degradation intensity *EAI* (wt. %) and Zr-containing vapors pressure p_v (Pa) for zirconium cathode material in the conditions of equilibrium and quasi-equilibrium systems ("air + CH_4"-mixture with the equivalence ratio ϕ = 1.71) (Tab. 1, 3)) at the temperature values of 2900 and 3100 K at *p* = 0.202 MPa

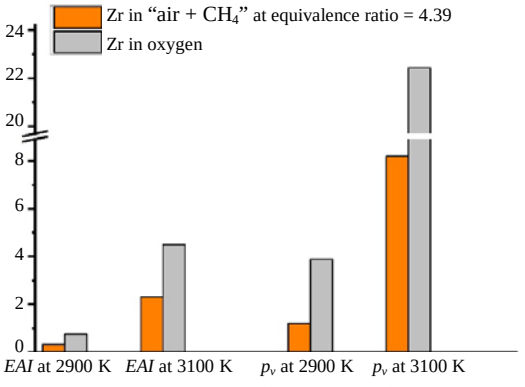

Fig. 8. Degradation intensity *EAI* (wt. %) and Zr-containing vapors pressure p_v (Pa) for zirconium cathode material in the conditions of two equilibrium systems (gaseous oxygen and "air + CH_4"-mixture with the equivalence ratio ϕ = 4.39 (Tab. 3 for the non-oxidative plasma regime, i. e. POX of C_xH_y) at the temperature values of 2900 and 3100 K at *p* = 0.202 MPa

It is inconsistent with the experimentally obtained in [17, 18] parameters of the cathode composition, which indicates a probability of none-quilibrium type of thermophysical and mass transfer processes in the near-electrode region and the surface layer (~1 mm thickness) of the material (at least when the torch operates in modes with electric current of about 300 A), which indicates the need for additional study of this effect.

Table 4

Combinations of the refractory (metal-based) cathode materials for DC arc plasma torches and some plasma gases, containing of hydrocarbons, and comparative ones, and calculated composition/state and the values of the (100 %–*EAI* (%))-parameter for evaporative degradation of the cathodes (at p = 0.202 MPa)

Material → Gas medium ↓	ThO_2-doped (2 wt. %) tungsten (T_1 = 3600 K)	Cu (at T_0 = 1300 K; for the oxidized state at T_1 = 1500 K)
1	2	3
Non-oxidative/weak oxidative plasmas – thermodynamic equilibrium and quasi-equilibrium cases		
1) N_2 (technical quality) – on the [50]	0 (for W + ThO_2 at 3000 K); 0.0271 (for W + ThO_2 at 3600 K) {at 300 K: WO_3(c) + ThO_2(c); at 3000 K: absence of phases: at 3600 K: W(c)}	–
2) N_2 (commercial grade) – high purity gas with minimal impurities [51]	0.96197** (for W + ThO_2 at 3000 K); 0.95387** (for W + ThO_2 at 3600 K) {at 300 K: W_2N(c) + + ThO_2(c); at 3000 K: W_2N(c); at 3600 K: W(c)}	0.99998 (at T = 1300 K) and 0.99994 (at T = 1350 K) and 0.9991 (at T = 1500 K)
3) N_2 (pure, 100 %)	0.97976** (for W + ThO_2 at 3000 K); 0.97034** (for W + ThO_2 at 3600 K) {at 300 K: W_2N(c) + + ThO_2(c); at 3000 K: W_2N(c); at 3600 K: W(c)}	–
4) Ar + H_2 (75 + 25 % vol.) (the commercial mixture for plasma spraying)	0.95213 (for W + ThO_2 at 3000 K); 0.94404 (for W + ThO_2 at 3600 K) {at 300 K: W(c) + + ThO_2(c); at 3000 K: W(c); at 3600 K: W(c)}	–
5) Air + C_3H_8 ≈ LPG* (at the equivalence ratio $\phi = 1/ER \approx 3.32$, i. e. ER = 0.3012), i. e. ideal POX	–	1.0 (at T = 1300 K) and 0.9999 (at T = = 1350 K) and 0.9982 (at T = 1500 K) (for all T exists only phase Cu(c))
6) Air + CH_4 (at $\phi = 1/ER$ = = 4.0, i. e. ER = 0.25), i. e. ideal POX	–	0.999949 (at T = 1300 K) and 0.999848 (at T = 1350 K) and 0.99787 (at T = 1500 K) (for all T exists only Cu(c))
7) N_2 (as #2) + + CH_4 (10 wt. %)	0.9666*** (for W + ThO_2) ≡ 0.94122 (for standardized value to the transformation as in #2); 0.9774*** (for W + ThO_2 at 3000 K) ≡ 0.95166 (for the standardized value) / (for the quasi-equilibrium regime the same result was found) {at 300 K: W_2N(c) + ThO_2(c); at 3000 K: WC(c); at 3600 K: WC(c)}	0.99996 (at 1300 K), 0.99989 (at 1350 K) and 0.99846 (at 1500 K) (for all T exists only Cu(c)) (†) / 0.99996 (at 1300 K), 0.99990 (at 1350 K) and 0.99849 (at 1500 K) (for all T exists only Cu(c)) (‡)
8) N_2 (as #3) + + CH_4 (10 wt. %)	0.9672*** (for W + ThO_2) ≡ 0.94179 (for standardized value to the transformation as in #2); 0.9778*** (for W + ThO_2 at 3000 K) ≡ 0.95213 (for the standardized value) {at 300 K: W_2N(c) + ThO_2(c); at 3000 K: WC(c); at 3600 K: WC(c)}	–
9) N_2 (as #3) + + CH_4 (20 wt. %)	0.96616*** (for W + ThO_2) ≡ 0.94077 (for standardized value to the transformation as in #2); 0.97783*** (for W + ThO_2 at 3000 K) ≡ 0.95213 (for the standardized value) {at 300 K: W_2N(c) + ThO_2(c); at 3000 K: WC(c); at 3600 K: WC(c)}	–
10) N_2 (as #3) + + C_3H_8 ≈ LPG* (10 wt. %)	0.96892*** (for W + ThO_2) ≡ 0.94346 (for standardized value to the transformation as in #2); 0.97783*** (for W + ThO_2 at 3000 K) ≡ 0.95213 (for the standardized value) {at 500 K: W_2N(c) + ThO_2(c) + C(c); at 3000 K: WC(c); at 3600 K: WC(c)}	–

Окончание табл. 4
End of Table 4

1	2	3
Oxidative plasmas – thermodynamic equilibrium case		
11) Air (composition on [48])	–	At Cu in initial mix: 1.000 (at T = = 1300–1350 K); 0.8994 ‡ ⁂ (at 1450 K) ≡ 0.999954 (for standardized value to the transformation as in (‡ ⁂)); and 0.8993 ‡ ⁂ (at 1500 K) ≡ 0.99987 (for the standardized value); at Cu_2O in initial mix: 1.000 (at T = 1300–1350 K); 0.8992 ‡ ⁂ (at 1450 K) ≡ 0.999952 (for the standardized value) and 0.8992 ‡ ⁂ (at 1500 K) ≡ 0.999851 (for the standardized value)
12) Air + CH_4 (at ϕ = = 1/ER = 1.00, i. e. ER = 1.00), i. e. ideal combustion	–	With standardizing to the Cu(c) state: 0.99998 (at 1300 K) and 0.99994 (at 1350 K) and 0.99899 (at 1500 K)⁂

Designation: † – thermodynamic equilibrium; ‡ – thermodynamic quasi-equilibrium; ‡ ⁂ – with CuO(c) → Cu_2O(c) transformation at high temperatures; ⁂ – with transformation of the part of Cu(c) to oxide (via the Cu(c) → Cu_2O(c) reaction) at high temperatures.
* LPG – liquified petroleum gas (technical propane-butane).
** With W_2N(c) → W(c) transformation at high temperatures.
*** With W_2N(c) → WC(c) transformation at high temperatures.

Besides the above described thermodynamic analysis, the tentative estimation was carried out for the comparative cathode metals degradation intensity to find the level of the degradation of the metal materials in terms of the vaporization part of the degradation based on the Hertz – Knudsen equation for the mass rate of the vaporization of metal and oxide melts [52]: $G_m = \alpha_{ec} p_v [M/2\pi RT]^{1/2}$.

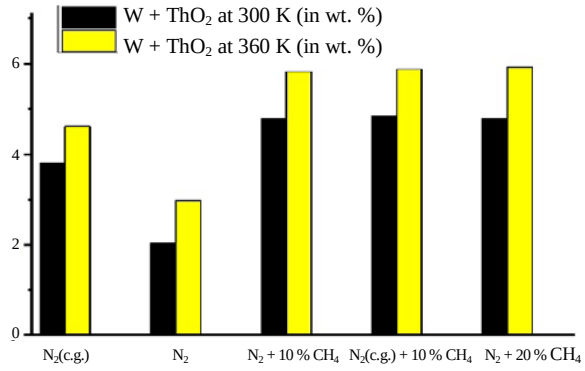

Fig. 9. Degradation intensity *EAI* (wt. %) for tungsten-based cathode material in different equilibrium systems with (W + ThO_2 (2 wt. %)), N_2 and CH_4 at the temperature values 3000 and 3600 K (at p = 0.202 MPa), according to Tab. 4, the modes are as follows: N_2 (c.g.) – commercial grade nitrogen [51]; N_2 – pure nitrogen (100 %)

In the above equation: α_{ec} – evaporation/condensation coefficient; M, p_v – molecular weight and the sum of partial pressures for the vapors of metal-containing components in gas; R – the molar gas constant. For the calculation such value α_{ec} was established, which can be found, as one of the variants [53], based on the Kincaid and Eyring approach for multiatomic liquids with use of the data for δ_3 – as the free angular ratio for non-linear molecules with three rotational degrees of freedom (characteristic for oxide and other melts). The values of α_{ec} in an accordance with the reviewed empirical data and some calculated ones for properties (M, p_v) near melting point of the materials was found to be 0.05–0.60 for a number of refractory oxides [52, 53].

As a result, we evaluated the data to compare the estimated erosion rate (in terms of evaporative part of this) for the thermochemical Zr-cathode when operating on the mixtures with AHC (such as "air + CH_4") with the same parameter for some known DC plasma torches with similar cathode materials [1, 3, 22, 54]. The values obtained show an agreement on the rate level (10^{-9}–10^{-8} g per Coulomb), which is important for engineering design of the AHC-based plasma torches at their medium or elevated power (≥50–100 kW).

The calculated thermodynamic data on the behavior of refractory zirconium compounds (such as ZrO_2, ZrC) under the C–H–O–N–Ar–Zr-system conditions at $T \geq 2500$ K can be also used for development of thermal protection systems to predict their ablation/destruction by vaporization in flows of combustion products (including incomplete combustion, i. e. with POX or pyrolysis) from various engine, turbine and rocket fuels.

CONCLUSIONS

1. The task stated was to evaluate approximate intensity of the erosion process and, in particular, the evaporation of cathode material of arc plasma torches for operation with gas mixtures with hydrocarbons by thermochemical modeling of the C–H–O–N–Ar–Me-system with varying operating parameters: the composition of plasma-forming mixtures, pressure and temperature of heterogeneous mixtures formed in the system with three variants of cathode material – zirconium, copper and commercial tungsten doped with thoria.

2. The calculations (according to the approach proposed by authors using the thermochemical method of the Bauman MGTU) for the conditions oriented to gas discharge chamber of DC plasma torch in the thermodynamic equilibrium approximation and with the deviation from equilibrium modes showed that the change in plasma type from the variants with oxidizing composition, such as a mixture of methane combustion products, to the variants of mixtures with reducing composition, gives the effect of a difference in the specific rate of vaporization of the cathode near the melting point of the cathode surface in a comparison with the case of the torch with N_2 or air. This effect is typical for two of the three materials considered (Zr and doped W).

3. With regard to the previously experimentally studied plasma torch with a zirconium cathode insert, operating in plasma in the thermochemical mode of electron emission [17, 18] and having an inhomogeneous multiphase surface, the calculation reveals a complex dependence of the specific vaporization rate of zirconium and the concentrations of Zr-containing compounds in the gas phase on the value of the fuel-air equivalence ratio of the plasma-forming CH_4-air mixture. This dynamics of the dependence differs from the data on the composition of surface layer in this cathode, which were established in experiments in the modes with electric current in the torch ~300 A, and this indicates nonequilibrium character of the processes in near-electrode plasma and in the surface layer of the electrode. During the modeling the specific erosion (assuming only its evaporative component) of a zirconium cathode in the "air + CH_4"-mixture was also compared with this parameter in experiments with previously studied plasma torches with similar cathodes of the thermochemical subgroup in other plasma gases.

4. The data obtained on the behavior of zirconium compounds ZrO_2 and ZrC in the C–H–O–N––Ar–Zr-systems are interesting for next design and optimizing the plasma torch cathodes and also for developing new Zr-containing thermal protection systems, including assessment of their destruction in flows of combustion products of a number of hydrocarbon-based fuels. Besides, the calculated results on the behavior of copper near its melting point can also be useful for analyzing the processes of thermal spraying of copper coatings.

REFERENCES

1. Zhukov M. F., Zasypkin I. M. (2007) *Thermal Plasma Torches: Design, Characteristics and Applications*. Cambridge (UK), Cambridge International Science Publ. 596.
2. Bielyi A. V., Kalinitchenko A. S., Devoino O. G., Kukareko V. A. (2017) *Surface Engineering of Structural Materials with Using of Plasma and Beam Technologies.* Minsk, Belorusskaya Nauka Publ. 457 (in Russian).
3. Petrov S. V., Saakov A. G. (2000) *Plasma of Combustion Products in Surface Engineering*. Kyiv, TOPAS Publ. 218 (in Russian).
4. Kornienko E. E., Mul' D. O., Rubtsova O. A., Vaschenko S. P., Kuzmin V. I., Gulyaev I. P., Sergachev D. V. (2016) Effect of Plasma Spraying Regimes on Structure and Properties of Ni_3Al Coatings. *Thermophysics and Aeromechanics*, 23 (6), 919–928. https://doi.org/10.1134/S0869 864316060147.
5. Petrov S. V. (1996) *Apparatus and Technological Principles of Coatings Thermal Spraying and Materials Processing in Gas-Air Plasma*. Kyiv, Gas Institute of NAS of Ukraine. 399 (in Ukrainian).
6. Korzhik V. N., Borisova A. L., Popov V. V., Kolomiitsev M. V., Chaika A. A., Tkachuk V. I., Vigilyanskaya N. V. (2014) Cermet Coatings of Chromium Carbide-Nichrome System Produced by Supersonic Plasma Gas Air Spraying. *The Paton Welding Journal*, (12), 19–24. https://doi.org/10.15407/tpwj2014.12.05.
7. Petrov S. V., Saakov A. G. (2002) Technology and Equipment for Plasma Surface Hardening of Heavy-Duty

Parts. *Materials and Manufacturing Processes*, 17 (3), 363–378. https://doi.org/10.1081/amp-120005382.
8. Martinez B., Mariaux G., Vardelle A. M., Barykin G., Parco M. (2009) Modeling and Control of a New Spray Process Combining Plasma and HVOF. *International Thermal Spray Conference (ITSC) 2009*. American Society for Metals. https://doi.org/10.1361/cp2009itsc0481.
9. Mohanty P. S., Roche A. D., Guduru R. K., Varadaraajan V. (2009) Ultrafine Particulate Dispersed High-Temperature Coatings by Hybrid Spray Process. *Journal of Thermal Spray Technology*, 19 (1–2), 484–494. https://doi.org/10.1007/s11666-009-9413-3.
10. Rita C. C. P., Miranda F. D. S., Caliari F. R., Rocha R. M., Essiptchouk A., Petraconi G. (2020) Hypersonic Plasma Setup for Oxidation Testing of Ultra-High Temperature Ceramic Composites. *Journal of Heat Transfer*, 142 (8), 082103. https://doi.org/10.1115/1.4047150.
11. Shen X., Gao N., Shi Z., Wang X., Zhang L., Huang J., Li K. (2021) New Insight into the Ablation Behavior of C/C-ZrC Composites in a Nitrogen Plasma Torch with a High Heat Flux of ~25 MW/m^2. *Corrosion Science*, 185, 109409. https://doi.org/10.1016/j.corsci.2021.109409.
12. Panakarajupally R. P., Mirza F., El Rassi J., Morscher G. N., Abdi F., Choi S. (2021) Solid Particle Erosion Behavior of Melt-Infiltrated SiC/SiC Ceramic Matrix Composites (CMCs) in a Simulated Turbine Engine Environment. *Composites. Part B: Engineering*, 216 (12), 108860. https://doi.org/10.1016/j.compositesb.2021.108860.
13. Bei G., van der Zwaag S., Kota S., Barsoum M. W., Sloof W. G. (2019) Ultra-High Temperature Ablation Behavior of MoAlB Ceramics Under an Oxyacetylene Flame. *Journal of the European Ceramic Society*, 39 (6), 2010–2017. https://doi.org/10.1016/j.jeurceramsoc.2019.01.016.
14. Maciel H. S., de Souza M. A., Gorbunov A. V., Miranda F. (2016) Demonstration Thermal Plasma System for the Treatment of Contaminated Ash Waste and WTE Applications. *Presentation for International Symposium on Non-Thermal/Thermal Plasma Pollution Control Technology & Sustainable Energy (ISNTP-10)*, August, 2016, Florianopolis, Brazil.
15. Ustimenko A. B. (2012) *Plasma-Fuel Systems for Increasing the Efficiency of the Using Solid Fuels*. Ulan-Ude, East Siberia State University of Technology and Management. 449 (in Russian).
16. Okovity V. A., Panteleenko F. I., Okovity V. V., Astashinsky V. M. (2020) Formation of Plasma Powder Coatings from Cermet with Subsequent High-Energy Modification. *Nauka i Technika = Science & Technique*, 19 (6), 469–474. https://doi.org/10.21122/2227-1031-2020-19-6-469-474 (in Russian).
17. Petrov S. V., Vasenin Yu. L. (2006) Behavior of the Arc at the Cathode in the Plasma of Combustion Products. *Tekhnologiya Mashinostroyeniya = Technology of Machine Industry*, (12), 41–44 (in Russian).
18. Petrov S. V., Saakov V. A., Vasenin Yu. L. (2004) Behaviour of the Arc at Cathode in Combustion Products Plasma. *31st EPS Conference on Plasma Physics, London, 28 June – 2 July 2004*. ECA, 28G, P-1.049.
19. Gorokhovski M., Karpenko E. I., Lockwood F. C., Messerle V. E., Trusov B. G., Ustimenko A. B. (2005) Plasma Technologies for Solid Fuels: Experiment and Theory. *Journal of the Energy Institute*, 78 (4), 157–171. https://doi. org/10.1179/174602205x68261.
20. Devoino O. G., Gorbunov A. V., Gorbunova V. A., Volod'ko A. S., Koval V. A., Yatskevich O. K., Halinouski A. A. (2021) Characterization of Opportunity for Upgrading of the System Based on Arc Plasma Torch for Thermal Spaying of Ceramic Materials, by Means of Use of Fuel Vortex Intensifier. Part I: Thermodynamic Modeling of the System Efficiency Parameters. *Vestsi Natsyyanal'nai Akademii Navuk Belarusi. Seryya Fizika-Technichnych Navuk = Proceedings of the National Academy of Sciences of Belarus. Physical-Technical Series*, 66 (4), 399–410. https://doi.org/10.29235/1561-8358-2021-66-4-399-410.
21. Essiptchouk A. M., Charakhovski L. I., Filho G. P., Maciel H. S., Otani C., Barros E. A. (2009) Thermal and Power Characteristics of Plasma Torch with Reverse Vortex. *Journal of Physics D: Applied Physics*, 42 (17), 175205. https://doi.org/10.1088/0022-3727/42/17/175205.
22. Anshakov A. S., Urbakh E. H., Urbakh A. E., Faleev V. A. (2005) Investigation of Thermochemical Cathodes in Arc Plasma Torches. *Teplofizika i Aeromekhanika = Thermophysics and Aeromechanics*, 12 (4), 685–691 (in Russian).
23. Gurvich L. V., Veyts I. V., Alcock C. B. (1988–1998) *Thermodynamic Properties of Individual Substances. Vols. 1–5*. 4th ed. New York, Hemisphere Publishing Co.
24. Methane. *NIST Chemistry WebBook*. Available at: https://webbook.nist.gov/cgi/cbook.cgi?ID=C74828&Units=SI&Mask=1#Thermo-Gas.
25. Lide D. R. (ed.) (2003) *CRC Handbook of Chemistry and Physics*. Bosa Roca, US, Taylor & Francis Inc. 2616.
26. Hafnium. Chemical Element. *Britannica*. Available at: https://www.britannica.com/science/hafnium.
27. Lassner E., Schubert W. D. (1999) *Tungsten: Properties, Chemistry, Technology of the Element, Alloys, and Chemical Compounds*. Springer Verlag Publ. https://doi.org/10.1007/978-1-4615-4907-9.
28. https://www.chemicalbook.com/ChemicalProductProperty_EN_CB5174366.htm.
29. Yan Z., Cai M., Shen P. K. (2013) Nanosized Tungsten Carbide Synthesized by a Novel Route at Low Temperature for High Performance Electrocatalysis. *Scientific Reports*, 3 (1), 1646. https://doi.org/10.1038/srep01646.
30. Tungsten Carbide. *PubChem*. Available at: https://pubchem.ncbi.nlm.nih.gov/compound/Tungsten-carbide# section=Chemical-and-Physical-Properties.
31. Hafnium Dioxide. *Webelements*. Available at: https://www.webelements.com/compounds/hafnium/hafnium_dioxide.html; Zirconium Dioxide. *Webelements*. Available at: https://www.webelements.com/compounds/zirconium/zirconium_dioxide.html; Copper Oxide. *Webelements*. Available at: https://www.webelements.com/compounds/copper/copper_oxide.html.
32. Ruh R., Garrett H. J., Domagala R. F., Tallan N. M. (1968) The System Zirconia-Hafnia. *Journal of the American Ceramic Society*, 51 (1), 23–28. https://doi.org/10.1111/j.1151-2916.1968.tb11822.x.
33. Backman L., Opila E. (2019). Thermodynamic Assessment of the Group IV, V and VI Oxides for the Design of Oxidation Resistant Multi-Principal Component Materials.

Journal of the European Ceramic Society, 39 (5), 1796–1802. https://doi.org/10.1016/j.jeurceramsoc.2018.11.004.
34. Jackson H. F., Jayaseelan D. D., Manara D., Casoni C. P., Lee W. E. (2011) Laser Melting of Zirconium Carbide: Determination of Phase Transitions in Refractory Ceramic Systems. *Journal of the American Ceramic Society*, 94 (10), 3561–3569. https://doi.org/10.1111/j.1551-2916.2011.04560.x.
35. Fernández Guillermet A. (1995) Analysis of Thermochemical Properties and Phase Stability in the Zirconium-Carbon System. *Journal of Alloys and Compounds*, 217 (1), 69–89. https://doi.org/10.1016/0925-8388(94)01310-e.
36. Sheindlin M., Falyakhov T., Petukhov S., Valyano G., Vasin A. (2018) Recent Advances in the Study of High-Temperature Behaviour of Non-Stoichiometric TaC_x, HfC_x and ZrC_x Carbides in the Domain of their Congruent Melting Point. *Advances in Applied Ceramics*, 117 (Suppl. 1), s48–s55. https://doi.org/10.1080/17436753.2018.1510819.
37. Justin J.-F., Julian-Jankowiak A., Guérineau V., Mathivet V., Debarre A. (2020) Ultra-High Temperature Ceramics Developments for Hypersonic Applications. *CEAS Aeronautical Journal*, 11 (3), 651–664. https://doi.org/10.1007/s13272-020-00445-y.
38. Ushakov S. V., Navrotsky A., Hong Q.-J., van de Walle A. (2019) Carbides and Nitrides of Zirconium and Hafnium. *Materials*, 12 (17), 2728. https://doi.org/10.3390/ma12172728.
39. Ma G., He P., Chen S., Kang J., Wang H., Liu M., Zhao Q., Li G. (2019) Physicochemical Properties of Yttria-Stabilized-Zirconia in-Flight Particles during Supersonic Atmospheric Plasma Spray. *Coatings*, 9 (7), 431. https://doi.org/10.3390/coatings9070431.
40. Suzuki M., Kagawa M., Syono Y., Hirai T. (1992) Synthesis of Ultrafine Single-Component Oxide Particles by the Spray-ICP Technique. *Journal of Materials Science*, 27 (3), 679–684. https://doi.org/10.1007/BF02403879.
41. Zirconium Carbide. *Chemical Book*. Available at: https://www.chemicalbook.com/ChemicalProductProperty_EN_CB6316307.htm.
42. Copper Oxide Powder. *IndiaMART*. Available at: https://www.indiamart.com/proddetail/copper-oxide-powder-21512086255.html.
43. Sillero J. A., Ortega D., Muñoz-Serrano E., Casado E. (2010) An Experimental Study of Thoriated Tungsten Cathodes Operating at Different Current Intensities in an Atmospheric-Pressure Plasma Torch. *Journal of Physics D: Applied Physics*, 43 (18), 185204. https://doi.org/10.1088/0022-3727/43/18/185204.
44. Quesne M. G., Roldan A., de Leeuw N. H., Catlow C. R. A. (2018) Bulk and Surface Properties of Metal Carbides: Implications for Catalysis. *Physical Chemistry Chemical Physics*, 20 (10), 6905–6916. https://doi.org/10.1039/c7cp06336a.
45. Hayami W., Tang S., Chiu T.-W., Tang J. (2021) Reduction in Work Functions of Transition-Metal Carbides and Oxycarbides upon Oxidation. *ACS Omega*, 6 (22), 14559–14565. https://doi.org/10.1021/acsomega.1c01671.
46. Singh B., Mehta B. R. (2014) Relationship Between Nature of Metal-Oxide Contacts and Resistive Switching Properties of Copper Oxide Thin Film Based Devices. *Thin Solid Films*, 569, 35–43. https://doi.org/10.1016/j.tsf.2014.08.030.
47. Deuermeier J., Liu H., Rapenne L., Calmeiro T., Renou G., Martins R., Munoz-Rojas D., Fortunato E. (2018) Visualization of Nanocrystalline CuO in the Grain Boundaries of Cu_2O Thin Films and Effect on Band Bending and Film Resistivity. *APL Materials*, 6 (9), 096103. https://doi.org/10.1063/1.5042046.
48. Rutberg P. G., Bratsev A. N., Kuznetsov V. A., Popov V. E., Ufimtsev A. A., Shtengel' S. V. (2011) On Efficiency of Plasma Gasification of Wood Residues. *Biomass and Bioenergy*, 35 (1), 495–504. https://doi.org/10.1016/j.biombioe.2010.09.01.
49. Atmospheric Concentrations of Greenhouse Gases. *EPA*. Available at: https://www.epa.gov/climate-indicators/climate-change-indicators-atmospheric-concentrations-greenhouse-gases#ref5.
50. State Standard 9293–74. ISO 2435-73. Gaseous and Liquid Nitrogen. Specifications. Moscow, Standartinform Publ. 1976 (in Russian).
51. Nitrogen Gas High Purity. *Krion*. Available at: https://krion.by/produktsiya/gazoobraznye-produkty-razdeleniya-vozdukha/azot-gazoobraznyy-vysokoy-chistoty.html (in Russian).
52. Shornikov S. I. (2015) Vaporization Coefficients of Oxides Contained in the Melts of Ca–Al-Inclusions in Chondrites. *Geochemistry International*, 53 (12), 1080–1089. https://doi.org/10.1134/s0016702915100055.
53. Gorbunov A. V. (1998) *Plasma Chemical Treatment of the Solutions of Nitrates of II–III Groups Metals in the Electric Arc Reactor*. Minsk, Heat & Mass Transfer Institute of NAS of Belarus. 332 (in Russian).
54. Kulygin V. M., Pereslavtsev A. B., Tresvyatsky S. S. (2017) Estimation of the Temporary Service Life of DC Arc Plasmatron Cathode. *Technical Physics*, 87 (9), 1327–1331. https://doi.org/10.1134/s1063784217090146.

Received: 20.07.2021
Accepted: 04.01.2022
Published online: 31.05.2022